Autonomous Navigation of a Quadcopter with Varying Payload Mass

-

Checkpoint 1

Gokul Prabhakaran
Department of Robotics
University of Michigan
Ann Arbor, Michigan, USA
Uniqname: gok

Federico Seghizzi
Department of Robotics
University of Michigan
Ann Arbor, Michigan, USA
Uniqname: seghizzi

I. Introduction

Across various industries, multi-rotor UAVs are slowly replacing helicopters for video-capture applications. Nonetheless, the latter still outperform the former in terms of goods transportation capabilities. In light of the recent development of ultra-high payload multi-rotor UAVs [1–3], this project aims to develop a framework that would enable the autonomous use of these vehicles for transportation and delivery purposes.

This project will focus on two key aspects of the problem: generating optimal trajectories through waypoints for the vehicle to complete its mission, and controlling the UAV's trajectory in spite of disturbances such as wind and varying mass. The perceptive behavior of the vehicle, combined with its ability to generate trajectories in response to it, are not considered as they are highly application-specific.

II. Vehicle Model

A. Vehicle

Throughout this project, a simple quad-rotor UAV with an X-configuration will be considered. This will be assumed to be left-right and forward-backward symmetric, with a payload case of fixed geometry hanging beneath its body. Figure 1 displays the assumed geometry for this quadcopter, along with its system diagram complete with inputs, outputs, and states.

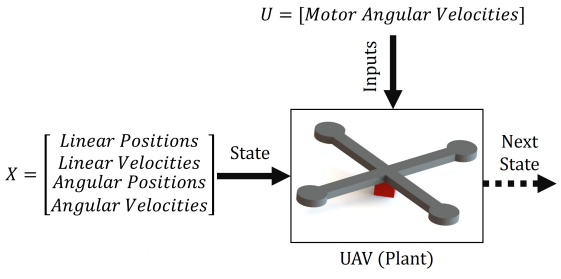

Fig. 1. Block diagram representation of the system, with inputs, outputs, and states.

The essential modeling parameters and constant for such a device are gathered in Table I. Given the focus of the project, the mass of the payload will be considered to vary both continuously and discontinuously as a function of time only; therefore this and the moments of inertia are not reported below.

TABLE I
Constants and parameters used for the quad-rotor analysis. Parameters with an * were taken from [4]. The remaining parameters were derived from computations or CAD software.

Symbol	Name	Value	Units
A_x	Vehicle area projected on the y-z body plane	$7.5e^{-3}$	m^2
A_y	Vehicle area projected on the x-z body plane	$7.5e^{-3}$	m^2
A_z	Vehicle area projected on the x-y body plane	$1.3e^{-2}$	m^2
l	Distance of the rotors from the CoM	$0.23*$	m
K_{rd}	Rotational drag coefficient (equal for all three axes)	$0.1*$	Nms
K_{td}	Translational drag coefficient (equal for all three directions)	0.62	kg/m^3
K_m	Moment coefficient for the rotor-prop combination	$7.5e^{-7}*$	Nms^2
K_f	Thrust coefficient for the rotor-prop combination	$3.13e^{-5}*$	Ns^2
g	Acceleration from gravity	9.81	m/s^2
m_{body}	Mass of the quad-rotor w/o payload	$0.65*$	kg

B. Reference Systems

Figure 2 shows the adopted frames of reference for the problem. The vehicle frame is chosen such that the positive X axis is aligned with the direction of forward flight, whilst the positive Z axis is aligned with the direction of thrust from the rotors. The origin of the frame is located in the center of mass (CoM) of the unloaded vehicle. In this frame, the rotational and translational velocity variables reported in Equation 1 are defined.

$$X_{TV} = \begin{bmatrix} u \\ v \\ w \end{bmatrix}, \quad X_{RV} = \begin{bmatrix} p \\ q \\ r \end{bmatrix} \tag{1}$$

As for the inertial frame, this is assumed to be tied to a point on Earth's surface, which is assumed to be flat and static. The Z axis points vertically upwards, in an equal but opposite direction to the acceleration due to gravity, whilst the X and Y lie on the plane of the Earth. In this frame, the rotational and translational displacement variables reported in Equation 2 are defined.

$$X_{TD} = \begin{bmatrix} x \\ y \\ z \end{bmatrix}, \quad X_{RD} = \begin{bmatrix} \phi \\ \theta \\ \psi \end{bmatrix} \tag{2}$$

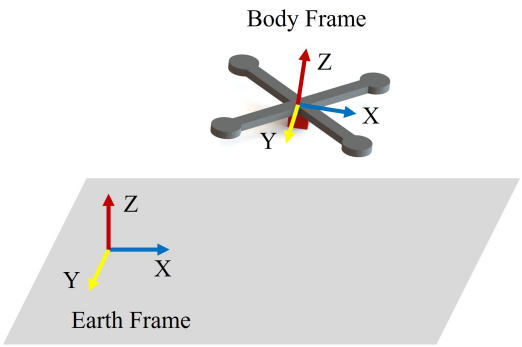

Fig. 2. Representation of the employed reference frames.

C. Equations of Motion

Given the above parameters and frames of reference, the Equations of Motion (EoM) can be written as shown in Equations 3 to 14.

1) Translation kinematic equations:

$$\dot{x} = u(c_\psi c_\theta) + v(c_\psi s_\theta s_\phi - s_\psi c_\phi) + w(c_\psi s_\theta c_\phi + s_\psi s_\phi) \tag{3}$$

$$\dot{y} = u(s_\psi c_\theta) + v(s_\phi s_\theta s_\phi + c_\psi c_\phi) + w(s_\psi s_\theta c_\phi - c_\psi s_\phi) \tag{4}$$

$$\dot{z} = u(-s_\theta) + v(c_\theta s_\phi) + w(c_\theta c_\phi) \tag{5}$$

2) Rotational kinematic equations:

$$\dot{\phi} = p + q(s_\phi t_\theta) + r(c_\phi t_\theta) \tag{6}$$

$$\dot{\theta} = q(c_\phi) - v(s_\phi) \tag{7}$$

$$\dot{\psi} = q(s_\phi sec_\theta) + v(c_\phi sec_\theta) \tag{8}$$

3) Translational dynamics equations:

$$\dot{u} = rv - pw + \frac{1}{m}(mgs_\theta - k_a A_v(\dot{x}_w - v)^2) \tag{9}$$

$$\dot{v} = pw - ru + \frac{1}{m}(-mgs_\phi c_\theta - k_a A_y(\dot{y}_w - v)^2) \tag{10}$$

$$\dot{w} = qv - pv + \frac{1}{m}(-mgc_\phi c_\theta + K_F \sum_{i=1}^{4} w_i^2 - k_a A_w(\dot{z}_w - w)^2) \tag{11}$$

Where $\dot{x}_w$, $\dot{y}_w$, and $\dot{z}_w$ are the body frame wind's velocity.

4) Rotational dynamics equations:

$$\dot{p} = \frac{1}{I_x}(lK_f(-w_1^2 - w_2^2 + w_3^2 + w_4^2)) - (I_z - Iy)qr - q\sum_{i=1}^{4} w_i - K_{D_x}p) \tag{12}$$

$$\dot{q} = \frac{1}{I_y}(lK_f(-w_1^2 + w_2^2 + w_3^2 - w_4^2)) - (I_x - I_z)pr + p\sum_{i=1}^{4} w_i - K_{D_y}q) \tag{13}$$

$$\dot{q} = \frac{1}{I_z}K_m(\sum_{i=1}^{4} w_i^2 - (I_{yy} - Ixx)qp - K_{D_z}r) \tag{14}$$

Note that, given the symmetry assumptions made above, the I_{xz}, I_{xy}, and I_{yz} terms are all zero and are not included.

D. Assumptions

The EoM reported above rest on a variety of important assumptions:

1) The vehicle is assumed rigid since the deflections it would experience would have a negligible effect on its motion.
2) The vehicle's propellers are assumed rigid since their short span would only result in minimum "flapping".
3) The vehicle is assumed perfectly left-right and forward-backward symmetric, given the numerous quadcopter designs featuring such characteristics.
4) The Earth is assumed flat and a valid inertial reference system, given the comparably small operating range, flight time, and cruising velocities of the quadcopter.
5) The acceleration due to gravity is assumed to be constant and uniform since its variations would have negligible effects on the quadcopter's motion.
6) The density of the atmosphere is assumed constant such that the thrust generated by the motors is constant for a given rotational velocity. This is acceptable given the reduced operating altitudes quadrotors typically operate in.
7) The motion of the atmosphere relative to the quadcopter is considered uniform at a given point in time. Additionally, it will be assumed that it can be comprehensively

expressed by a set of velocity vectors in either the inertial or body frames. This is acceptable given the quadcopter's small scale relative to atmospheric phenomena.

8) The vehicle is assumed to be subject exclusively to aerodynamic drag, gravitational, thrust, and gyroscopic effects, acting as expressed in Section II.B and II.C.
9) Given the limited roll, pitch, and yaw rates, the gyroscopic effects of the entire quadcopter's rotation are assumed negligible.
10) The reference frames are assumed to be oriented as expressed in Section II.B.

III. Linearization

Given the nonlinear EoM presented above, the system had to be linearized to simplify the development of an effective controller.

A. Equilibrium Point

The equilibrium point selected for linearizing the system was the hover condition. In this condition, state variables are set to 0, and control inputs are set to perfectly compensate for the weight of the UAV:

$$X_{eq} = 0^{12\times 1}, \quad U_{eq} = \sqrt{\frac{mg}{4k_f}} \begin{bmatrix} 1 \\ 1 \\ 1 \\ 1 \end{bmatrix} \tag{15}$$

This condition is the trivial equilibrium condition, as it can easily be seen that it will ensure all EoM presented in Section II.C go to zero. Whilst other equilibrium points may exist, in practice this condition is used even when developing complex controllers [4, 5]. Furthermore, given the specific application of the quad-copter, this is unlikely to experience large angles or velocities which would push the system meaningfully far from the linearization point. Alternative equilibria were thus not considered.

B. Linearized System

Given the above equilibrium condition, the system was linearized by simply taking the jacobians of the EoM with respect to the state vector and the control vector, and evaluating said jacobians with the values in Equation 15. This produced the system system reported in Equation 16, with the A and B matrices defined as in Equation 17 and 18.

$$\dot{X} = A \cdot X + B \cdot U \tag{16}$$

C. Open-Loop System Comparison

To evaluate whether the linearized system reported in Equation 16 performed similarly to its non-linearized counterpart in Equations 3 to 14, the two were simulated assuming no payload mass or payload mass variation, and no wind. The initial conditions and fixed inputs employed for these simulations are reported in Table II. Whilst limited for most quadcopters, these maneuvers are what a transport/delivery UAV strictly needs to perform to successfully complete its mission, and are therefore deemed appropriate given the scope of the project. Results for the open-loop simulations are presented in Figures 3 to 5, where each state variable is plotted against time for both models.

TABLE II
Open-loop initial conditions and control inputs for common quadcopter maneuvers. Only non-zero initial conditions for the state vector are specified.

Description	$\mathbf{X(0)}$	$\mathbf{U}$
Static Hover	All Zeros	$u_{1,2,3,4} = 225.00 rad/s$
Steady Ascent	$w = 1 m/s$	$u_{1,2,3,4} = 225.50 rad/s$
Steady Straight Flight	$u = 2 m/s$, $w = 7.8e^{-3} m/s$, $\theta = 0.22°$	$u_{1,2,3,4} = 224.99 rad/s$

As can be seen, the linearized model can somewhat adequately predict the performance of the non-linearized model. Specifically, the linearized model's states are at most $\sim 5\%$ off from their non-linearized counterpart for every second of simulation. Whilst this could become very significant over long maneuvers, it is an inherent and unavoidable limitation of the linearization of the numerous square velocities terms within the system. Overall, however, since the maneuvers and limited velocities needed for a transport or delivery-focused quadcopter are unlikely to exceed those presented above, the model is likely acceptable for this project

IV. Performance

A. Stability Analysis

Given the viability of the above-presented linearized system, its stability had to be evaluated. This was done by evaluating the eigenvalues of the A matrix, as reported in Equations 19 to 21. The corresponding eigenvectors are impractical to report and will be thus simply described qualitatively.

$$\lambda_1 = \frac{-0.1}{I_z} \tag{19}$$

$$\lambda_{2,3} = -\frac{I_x + I_y \pm \sqrt{(I_x^2 + I_y^2 - 3.24e^{+8} I_x I_y)}}{20 I_x I_y} \tag{20}$$

$$\lambda_{4-12} = 0 \tag{21}$$

Considering each eigenvalue:

- λ_1: This eigenvalue will always have a real negative value, and represents stable non-oscillatory behavior. The corresponding eigenvector has terms associated only with the ψ and r, suggesting any disturbances to these states die down and the system will return to its equilibrium.
- $\lambda_{2,3}$: These eigenvalues will always be a complex conjugate pair with a negative real part, translating to a damped oscillatory behavior. Considering the associated eigenvectors, these have terms for the x, y, u, v, ϕ, θ, p, and q states, although the latter two are at least 6

$$A = \begin{bmatrix} 0 & 0 & 0 & 1 & 0 & 0 & 0 & 0 & 0 & 0 & 0 & 0 \\ 0 & 0 & 0 & 0 & 1 & 0 & 0 & 0 & 0 & 0 & 0 & 0 \\ 0 & 0 & 0 & 0 & 0 & 1 & 0 & 0 & 0 & 0 & 0 & 0 \\ 0 & 0 & 0 & 0 & 0 & 0 & 0 & 9.81 & 0 & 0 & 0 & 0 \\ 0 & 0 & 0 & 0 & 0 & 0 & -9.81 & 0 & 0 & 0 & 0 & 0 \\ 0 & 0 & 0 & 0 & 0 & 0 & 0 & 0 & 0 & 0 & 0 & 0 \\ 0 & 0 & 0 & 0 & 0 & 0 & 0 & 0 & 0 & 1 & 0 & 0 \\ 0 & 0 & 0 & 0 & 0 & 0 & 0 & 0 & 0 & 0 & 1 & 0 \\ 0 & 0 & 0 & 0 & 0 & 0 & 0 & 0 & 0 & 0 & 0 & 1 \\ 0 & 0 & 0 & 0 & 0 & 0 & 0 & 0 & 0 & \frac{-0.1}{I_x} & -\frac{4(\sqrt{78355m})}{I_x} & 0 \\ 0 & 0 & 0 & 0 & 0 & 0 & 0 & 0 & 0 & \frac{4\sqrt{78355m}}{I_y} & \frac{-0.1}{I_y} & 0 \\ 0 & 0 & 0 & 0 & 0 & 0 & 0 & 0 & 0 & 0 & 0 & \frac{-0.1}{I_z} \end{bmatrix} \tag{17}$$

$$B = \begin{bmatrix} 0 & 0 & 0 & 0 \\ 0 & 0 & 0 & 0 \\ 0 & 0 & 0 & 0 \\ 0 & 0 & 0 & 0 \\ 0 & 0 & 0 & 0 \\ \frac{6.26e^{-5}\sqrt{78355m}}{m} & \frac{6.26e^{-5}\sqrt{78355m}}{m} & \frac{6.26e^{-5}\sqrt{78355m}}{m} & \frac{6.26e^{-5}\sqrt{78355m}}{m} \\ 0 & 0 & 0 & 0 \\ 0 & 0 & 0 & 0 \\ 0 & 0 & 0 & 0 \\ \frac{-1.44e^{-5}\sqrt{78355m}}{Ix} & \frac{-1.44e^{-5}\sqrt{78355m}}{Ix} & \frac{1.44e^{-5}\sqrt{78355m}}{Ix} & \frac{1.44e^{-5}\sqrt{78355m}}{Ix} \\ \frac{-1.44e^{-5}\sqrt{78355m}}{Iy} & \frac{1.44e^{-5}\sqrt{78355m}}{Iy} & \frac{1.44e^{-5}\sqrt{78355m}}{Iy} & \frac{-1.44e^{-5}\sqrt{78355m}}{Iy} \\ \frac{1.5e^{-6}\sqrt{78355m}}{Iz} & \frac{-1.5e^{-6}\sqrt{78355m}}{Iz} & \frac{1.5e^{-6}\sqrt{78355m}}{Iz} & \frac{-1.5e^{-6}\sqrt{78355m}}{Iz} \end{bmatrix} \tag{18}$$

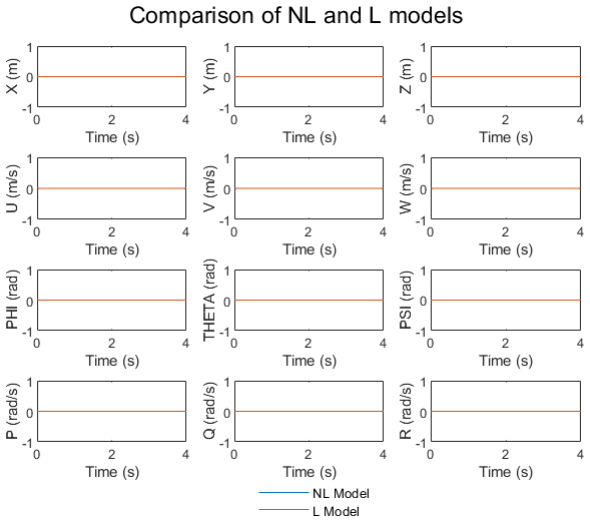

Fig. 3. Comparison between Linear and Non-Linear Quadcopter models for a hover condition.

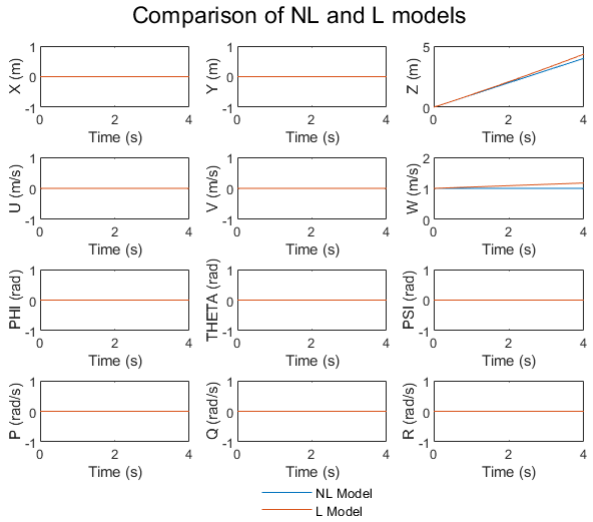

Fig. 4. Comparison between Linear and Non-Linear Quadcopter models for a steady-state ascent condition.

orders of magnitude greater than the former, indicating their dominance in the mode of oscillation. Disturbances in these two states are expected to decay after some oscillations.

- λ_{4-12}: The eigenvalue of 0 is repeated nine times, and represents critically stable behaviour. If the system is disturbed along the specific or generalized eigenvectors, it will simply settle at the disturbed value.

Based on the above, it can be said that the system is at best critically stable.

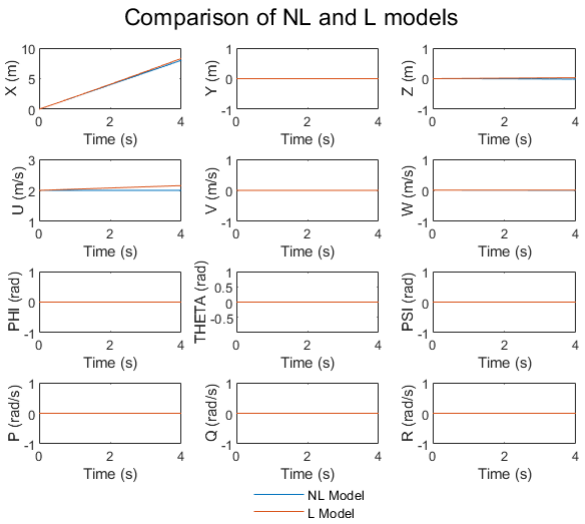

Fig. 5. Comparison between Linear and Non-Linear Quadcopter models for a steady straight flight condition.

B. Controllability Analysis

To develop a controller that compensates for this critically stable behavior, the controllability of the system must be considered. This was evaluated through a Popov–Belevitch–Hautus (PBH) Test [6], which confirmed that all 12 modes are controllable, suggesting that the system is fully controllable.

Notably, comparing this result against other tests for controllability, discrepancies emerged. Specifically, when considering the rank of the controllability matrix, this was found to be 2 if using the "crtb" MATLAB function, or 10 if computing the matrix by hand. These discrepancies are likely due to the specific numerical tolerances MATLAB employs when computing the ranks in each of these tests. Consequently, this means that whilst the system may theoretically be fully controllable, practically it may be comparatively unresponsive when attempting to control specific modes.

To attempt to quantify this, Table III reports the tolerance needed in MATLAB for a specific eigenvalue to pass the PBH test. Linearization point, mass, and inertial terms considered were set to match what was used in Section III.C

TABLE III
TOLERANCE NEEDED FOR EACH EIGENVALUES TO PASS THE PBH TEST.

Eigenvalue	Tolerance
$\lambda_{2,3}$	e^{-1}
λ_1	e^{-2}
λ_{4-12}	e^{-6}

C. Disturbances

Given the system presented above, the controller to be designed will attempt to both stabilize the critically stable modes and equally compensate for the effects of wind and mass variation.

The mass, and associated inertia terms, will be varied according to Equations 22 and 23, capturing both discontinuous and continuous variations. Wind velocity in the three directions will be similarly varied according to Equation 24.

$$m_{total} = \begin{cases} m_{body} + m_{payload}, & \text{if } 0 <= t <= t_{drop} \\ m_{body}, & \text{otherwise} \end{cases} \tag{22}$$

$$m_{total} = m_{body} + k_{mass}t \tag{23}$$

$$\begin{bmatrix} \dot{x}_w \\ \dot{y}_w \\ \dot{z}_w \end{bmatrix} = \begin{cases} \begin{bmatrix} k_{wind}t + \dot{x}_{gust} \\ k_{wind}t + \dot{y}_{gust} \\ k_{wind}t + \dot{z}_{gust} \end{bmatrix}, & \text{if } t = t_{gust} \\ \begin{bmatrix} k_{wind}t \\ k_{wind}t \\ k_{wind}t \end{bmatrix}, & \text{otherwise} \end{cases} \tag{24}$$

Where k_{mass} and k_{wind} are constants dictating the continuous rate of change; $m_{payload}$ is the mass of a droppable payload; $\dot{x}_{gust}$, $\dot{y}_{gust}$, $\dot{z}_{gust}$ refers to the additional wind velocity due to a gust.

REFERENCES

[1] Griff aviation. https://www.griffaviation.com/. Accessed October 2, 2023.

[2] Draganfly inc. - heavy lift uav. https://draganfly.com/products/heavy-lift/. Accessed October 2, 2023.

[3] Freefly systems - alta x. https://freeflysystems.com/alta-x. Accessed October 2, 2023.

[4] M. Islam, M. Okasha, and M. M. Idres, "Dynamics and control of quadcopter using linear model predictive control approach," *IOP Conference Series: Materials Science and Engineering*, vol. 270, p. 012007, 2017.

[5] R. Kumar, M. Bhargavapuri, A. M. Deshpande, S. Sridhar, K. Cohen, and M. Kumar, "Quaternion feedback based autonomous control of a quadcopter uav with thrust vectoring rotors," in *2020 American Control Conference (ACC)*, 2020, pp. 3828–3833.

[6] B. Gillespie. (2020) PBH Tests - ME564 - Linear Systems Theory. University Name. [Online]. Available: https://umich.instructure.com/courses/548697/external$_tools/53084$